Hessisches Kompetenzzentrum
für Hochleistungsrechnen

An Agent-Based Model of Radiation-Induced Lung Fibrosis

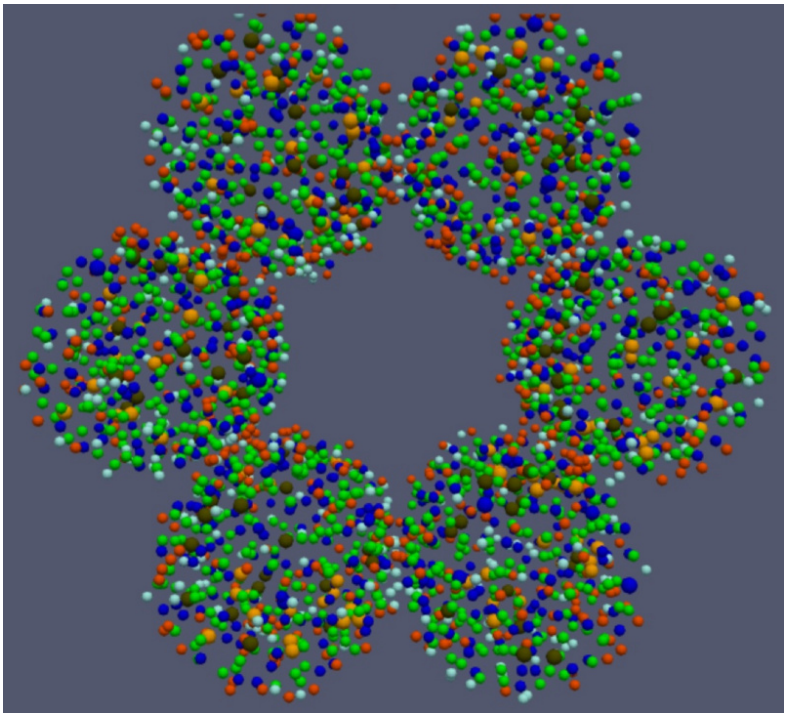

Project Manager
Nicolò Cogno

Researchers
Dr. Roman Bauer

Principal Investigator
Prof. Marco Durante

Project Term
2022 - 2023

Clusters
Lichtenberg II Cluster Darmstadt

Additional Software
BioDynaMo

Institute
Institute for Condensed Matter Physics

University
Technische Universität Darmstadt

Introduction

Radiation-induced lung injuries such as pneumonitis and lung fibrosis (RILF) can lead to respiratory failure and eventually death. Moreover, they impose significant constraints on the maximum dose and irradiated volume in thoracic radiotherapy. Currently, normal tissue complication probability (NTCP) models for organs at risk rely on clinical experience to set tolerance doses, without a mechanistic understanding of the underlying processes.
To address these challenges, we developed a 3D agent-based model (ABM) that simulates cell dynamics and substance diffusion following radiation injury in an alveolar duct. In this context, the use of an high performance computer (HPC) can shorten simulation times and simplify sensitivity analyses by allowing parallel testing of different parameter values. Furthermore, ABMs are aimed at simulating systems of many interacting entities. Their intrinsic nature thus makes HPCs well-suited architectures for ABM simulations as they can strongly benefit from multiple cores as well as multithreading.

Methods

Our model replicates a human alveolar duct where spherical agents represent alveolar cells. Depending on their type, cells in our model are assigned behaviours when they are added to the

simulation and sequentially perform the prescribed activities until they are removed. The main behavior categories are the following: secretion, damage spreading and clearance, migration, proliferation, differentiation and apoptosis.
The radiation damage in our model is simulated as depletion of healthy type 2 alveolar epithelial cells (AEC2). To simulate an heterogeneous damage, depleted fractions for each alveolus are drawn from Poisson distributions centred on the average number of injured cells for a given dose. For each dose, the surviving fraction is estimated by fitting experimental data from a study on rats' AEC2.

Results

A significant increase in the ECM concentration was observed at 3 months following the irradiation due to the spread of the senescent AEC2 and the consequent rise in the number of mesenchymal cells. The clearance of the senescent cells reduced the inflammation, and the homeostatic conditions were restored for the alveoli irradiated at doses < 5 Gy circa. Although all the senescent AEC2 were eventually removed for each dose, some alveoli were fully depleted from the AEC2 and underwent a permanent increase in the ECM. Our results, showing two distinguishable fibrotic responses, an early and a late one, are consistent with patterns detected in human lungs irradiated with photons. Moreover, the time-to-peak for the early response matches quantitative experimental data reported in the literature. Finally, a good agreement was observed between the increase in ECM concentration as a function of the delivered dose and previously published experimental results.
We fitted our data using the survival curve from the critical volume model and discrepancies were found between our data and the given model, with lower survival predicted by the model for the doses at the higher end of the simulated range. We suppose that the cause of this difference is the AEC2 repopulation not being compensated by the bystander senescence mechanism.
We introduced a custom indicator, the RSI, as a surrogate measure of the RILF severity. The RSI is a positive number that measures the fibrosis damage by combining the depletion of the alveoli with the increase in the average concentration of the ECM. We computed the reduction in the functioning lung tissue as the loss of the volume due to the depleted alveoli and measured the average rise in the ECM concentration with respect to the homeostatic values. The results show quantitative agreement with the model parameters published in a previous study. Taken together, these outcomes support the RSI as an alternative to the fibrosis index for computational simulations where a direct measure of the decrease in the functioning volume might not be available.
We measured the alveoli survival with multiple senescent-to-damaged ratios when irradiated at different doses. Lowering the fraction of senescent AEC2 increased the alveoli survival at the same dose. Notably, this feature could be exploited to simulate the effects of senolytic drugs on lung tissue, which have been shown to be able to reverse persistent RILF and IPF in mice.

Discussion

We implemented an ABM of a human alveolar segment and simulated the onset of RILF after the irradiation with single-fraction X-rays. We downscaled the model presented in our previous work to the cellular level and added key cellular behaviours that have been documented both in RILF and IPF, such as cell repopulation, senescent cells clearance, and bystander senescence. Our study emphasizes the role of cellular and molecular mechanisms in NTCP modelling and shows the time evolution of the RILF status. After testing several combinations of the bystander threshold parameter and phagocytic fraction, we set them to 2 and 100%, respectively. When using these values, we observed full clearance of the senescent cells and epithelial recovery at doses <5 Gy, as shown in a previous experimental study.
This study showed that the model could replicate results published in the literature and highlighted discrepancies between the alveoli survival predicted by the critical volume model and our simulations. Contextually, we draw attention to the importance of both cell–cell and cell–environment interactions which introduce a time dependence in the survival curve of the alveolar stem cells.
Finally, our work could set the basis for modelling and testing the modulation of NTCP when RT is combined with drugs. Such models could then be exploited to optimize the treatments as a step towards personalized medicine.

Figures

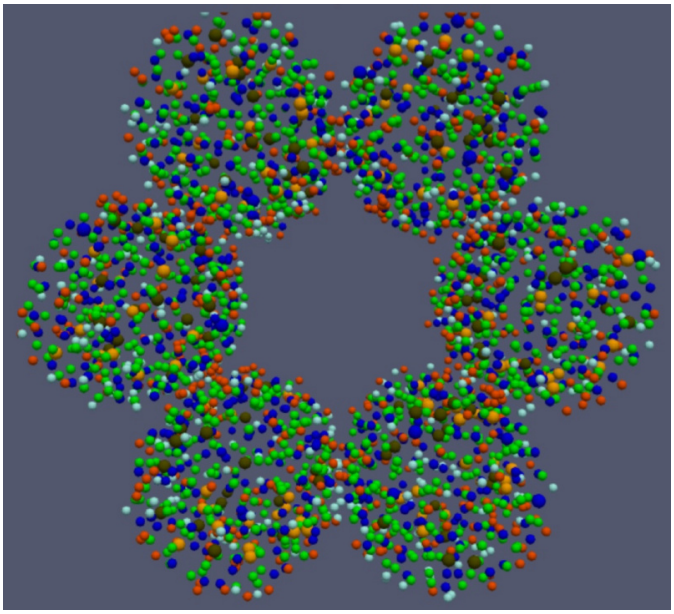

Figure 1: Visual output of the 3D ABM of a human alveolar duct. The structure is made up of 3 stacked layers, and each layer consists of 6 tangent alveoli. The centres of the alveoli are located on equidistant circles with a radius equal to the duct radius. Cells are represented as coloured spheres, with green = AEC2 cells, blue = AEC1 cells, brown = M1 macrophages, orange = M2 macrophages, light blue = fibroblasts, red = myofibroblasts.

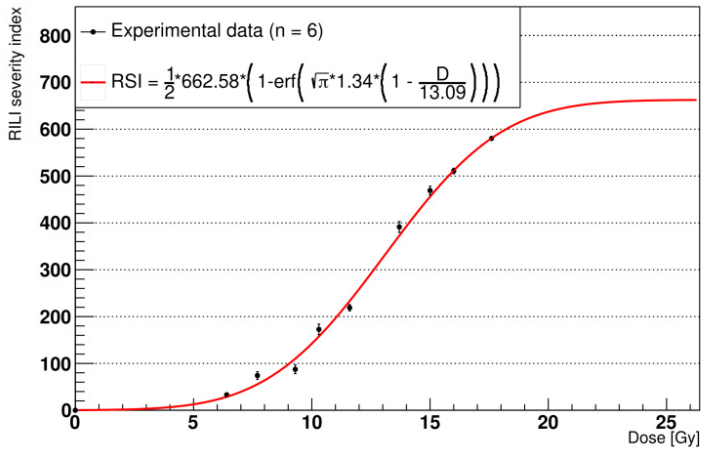

Figure 2: RILI severity index after 1000 days with phagocytic fraction = 100% (n = number of experiments).

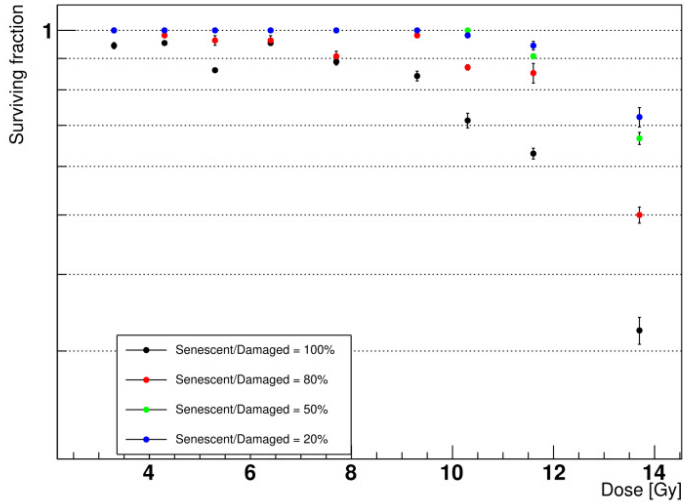

Figure 3: Alveoli survival after 1000 days with phagocytic fraction = 100% and different senescent to damaged AEC2 ratios. Senescent/Damaged = x% means that, after the irradiation, a fraction x of the healthy AEC2 shifted to the senescent state, while the remaining 1 − x fraction underwent apoptosis.

Publications

Cogno, N.; Bauer, R.; Durante, M. An Agent-Based Model of Radiation-Induced Lung Fibrosis. Int. J. Mol. Sci. 23, 13920 (2022) https://doi.org/10.3390/ijms232213920

Last Update: 2023-05-25 15:18